[溶接学会論文集　第 27 巻　第 2 号　p. 4s-7s（2009)]

Numerical Analysis of Metal Vapor Behavior with Multi-diffusion System in TIG Welding of Stainless Steel*

by Kentaro Yamamoto**, Manabu Tanaka***, Shinichi Tashiro***, Kazuhiro Nakata***, Kei Yamazaki****,

Eri Yamamoto****, Keiichi Suzuki**** and A. B. Murphy*****

In the present paper, a TIG arc in helium or argon is modeled taking into account the contamination of the plasma by the metal vapor from a stainless-steel weld pool. Iron, chromium and manganese are considered as the metal vapor species in this model. A viscosity approximation is used to express the diffusion coefficient in terms of the viscosities of the shielding gas and the metal vapor. The time-dependent two-dimensional distributions of temperature, velocity and metal vapor concentrations of iron, chromium and manganese are predicted, together with the weld penetration as a function of time for a 150 A arc at atmospheric pressure, for both helium and argon shielding gases. The distribution of the metal vapors depends on the diffusion term and the convection term. Due to the cathode jet, the convection term has a strong effect. Consequently, it is found that the metal vapors expand in the radial direction and are concentrated around the weld pool surface. The concentration of manganese vapor is larger than those of iron and chromium vapors, despite the fact that the proportion of manganese in stainless steel is significantly smaller.

Key Words: Arc, Welding, Stainless steel, Metal vapor, Numerical simulation

1. Introduction

During the arc welding process, four states of matter, solid, liquid, gas and plasma, simultaneously exist and mutually interact within a volume of only 1 cm^3. The temperature range is wide, ranging from about 20000 K in the arc plasma, about 3000 K in the tungsten cathode, about 2000 K in the molten steel, down to room temperature in the surrounding regions[1]. Due to the remarkable progress in computer simulation and observation techniques recently, it has become possible to understand the phenomena in arc welding processes quantitatively[2, 3]. However, it has not been possible to accurately predict the welding parameters, such as the arc voltage and the weld geometry. It is known empirically that the arc voltage in TIG arc on water-cooled copper differs from that in TIG arc welding. This phenomenon is caused by the metal vapor from the weld pool surface. For a full understanding and accurate prediction of these parameters, it is necessary to understand the behavior of metal vapor in the arc plasma.

Metal atoms generally have more low-energy excited states, and are more easily ionized, than atoms of shielding gases such as argon and helium. These characteristics contribute to an increase of the radiative emission coefficient and the electric conductivity of the plasma. It is estimated that the former affects the thermal pinch effect and the energy efficiency of the arc plasma and that the latter affects the current density distribution. Tashiro et al[4] conducted a virtual experiment by numerical simulating a pure helium arc and an arc in helium uniformly mixed with 30 mol% iron atoms, and showed that an obvious arc constriction occurred for the latter case. Furthermore, they reported that the energy efficiency greatly decreased from about 80% to about 35%. These results suggested that existence of metal vapor changed the heat source property in the arc welding process, and consequently changed the size and the shape of the molten pool.

As noted above, there have been significant advances in the simulation of the arc welding. For example, a numerical simulation of gas metal arc welding, including the formation of droplets from a steel wire electrode, has been reported[5]. However, the shielding gas was pure argon, and the effect of metal vapor was not considered. On the other hand, calculations of the behavior of metal vapor in an atmospheric pressure plasma have also been reported[6]. However, the conditions were far from those of welding because a solid electrode with constant temperature was assumed. It is important for accurate understanding of the arc welding process to consider the mixing of the metal vapor in a model that takes into account the tungsten cathode, the arc plasma and the weld pool.

Authors developed a numerical model of stationary TIG arc welding taking into account the metal vapor produced from the weld pool surface[7]. The anode was assumed to be a stainless steel. In practice, metal vapor species in an arc plasma with a stainless steel anode include Fe, Cr, Ni, Mn and so on[8]. However, only iron vapor was considered in the model.

*Received: 2008.11.18
**Student Member, Graduate school, Osaka University
***Member, Joining and Welding Research Institute Osaka University
****Welding Company, Kobe Steel, Ltd.
*****CSIRO Materials Science and Engineering

In the present paper, we use a numerical model of stationary TIG arc welding taking into account the iron, chromium and manganese vapors produced from the weld pool surface, and we simulate the distribution of the metal vapors, the plasma temperature, fluid flow velocity and the formation of the weld pool.

2. Simulation model

The tungsten cathode, arc plasma and anode are described relative to cylindrical coordinates, assuming rotational symmetry around the arc axis. The calculation domain is shown in figure 1. The diameter of the tungsten cathode is 3.2 mm with a 60 degrees conical tip. The anode is of a stainless steel and composition for a stainless steel in the present model is given in table 1. Helium shielding gas is introduced from the outside of the cathode on the upper boundary at the flow rate of 30 L/min.

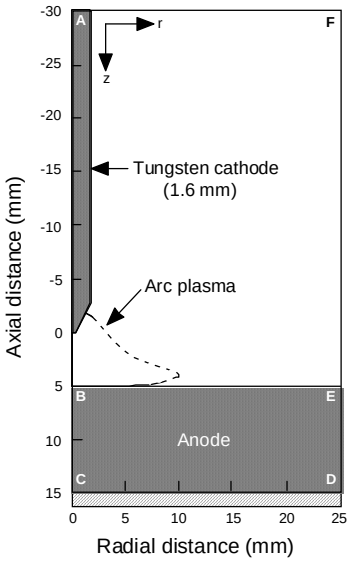

Fig. 1 Schematic illustration of simulation domain.

Table 1 Composition for a stainless steel used in the model

Fe	Cr	Mn
80.5 wt%	18.0 wt%	1.5 wt%

The convection in the weld pool is influenced by the shear stress due to the convective flow of the cathode jet, the Marangoni force due to the gradient in the surface tension of the weld pool, buoyancy due to gravity and the electromagnetic pinch force due to the arc current. Only the driving forces of the weld pool convection at the boundary between the weld pool and the arc plasma are explained here. First, the shear stress is already included in radial momentum conservation through the viscosity at the anode surface. Second, the Marangoni force is given by[9)]

$$M_A = \frac{\partial}{\partial z}\left(\frac{\partial \gamma}{\partial T}\frac{\partial T}{\partial r}\right) \tag{1}$$

where T is temperature, γ is the surface tension of the weld pool. In this paper, stainless steel is assumed to have low sulfur content (about 10 ppm) and the variation of the surface tension at the weld pool surface is assumed to decrease linearly with increasing temperature ($\partial\gamma/\partial T = -0.46 mN/mK$) [9)].

A species conservation equation expressed by Eq. (2) is applied to take into account the metal vapors behavior[6)]. Iron, chromium and manganese vapors are considered in this model. However, to simplify the model and facilitate calculation, those vapors are not calculated simultaneously but are calculated separately, as He-Fe, He-Cr and He-Mn system.

$$\frac{\partial}{\partial t}(\rho C_i) + \frac{1}{r}\frac{\partial}{\partial r}(r\rho v_r C_i) + \frac{\partial}{\partial z}(\rho v_z C_i) = \frac{1}{r}\frac{\partial}{\partial r}\left(r\rho D_i \frac{\partial C_i}{\partial r}\right) + \frac{\partial}{\partial z}\left(\rho D_i \frac{\partial C_i}{\partial z}\right) \tag{2}$$

where t is time, v_r and v_z are the radial and axial velocities, ρ is the density, C_i is mass fraction concentration of metal vapor and D_i is the binary diffusion coefficient, which is expressed by the viscosity approximation equation:

$$D_i = \frac{2\sqrt{2}\left(1/M_i + 1/M_g\right)^{0.5}}{\left[\left(\rho_i^2/\beta_i^2\eta_i^2 M_i\right)^{0.25} + \left(\rho_g^2/\beta_g^2\eta_g^2 M_g\right)^{0.25}\right]^2} \tag{3}$$

where M_i and M_g are the molecular weights of metals and the shielding gas respectively. Similarly, ρ_i, ρ_g, η_i, η_g are respectively the density and viscosity of metals and the shielding gas. β_i, β_g are the dimensionless constant defined as $\beta_i = (D_{ii}\rho_i)/\eta_i$, and theoretically range 1.2 to 1.543 for various species of gas, such as Ar, He, H_2, N_2, O_2, CO_2 and so on. It is assumed that $\beta_i = \beta_g = 1.385$, which is based on the mean value of experimental data[10)]. The viscosity approximation is not strictly justified since it does not take into account ionized species and is at best reasonably accurate[11)]; however it is considered to be a useful first approximation for the arc welding model.

C_i is set to be zero in the cathode area and in the solid area of the anode. However, at the anode surface where the temperature is above the melting point, C_i is set to[6)]:

$$C_i = \frac{n_i p_{v,i} M_i}{n_i p_{v,i} M_i + \left(p_{atm} - n_i p_{v,i}\right) M_g} \tag{4}$$

where p_{atm} is atmospheric pressure and $p_{v,i}$ is the partial pressure of metal vapor, which is a function of the weld pool temperature[12)], and n_i is mol fraction of a metal in stainless steel.

According to Eq. (4), C_i has values between zero and 1.0. For other boundary conditions, C_i=0 at AF and FE shown in Fig. 1, and $(\partial C_i/\partial r)=0$ at the arc axis (AB)

In the present model, plasma properties are dependent on not only the temperature but also the mole fraction of iron, chromium and manganese vapors. However, iron, chromium and manganese vapors are all considered as iron vapor in calculating plasma properties for the simplification. Plasma properties at intermediate concentrations of iron vapor are calculated using a linear approximation based on the properties at 0 mol%, 1 mol%, 10 mol%, 20 mol% and 30 mol%[13]. The properties were calculated assuming the arc plasma to be in the local thermodynamic equilibrium (LTE), and using the Chapman-Enskog approximation[13]. For example, the electrical conductivities, which are significantly affected, are shown in Fig. 2. The electrical conductivities are greatly increased by the addition of iron vapor at temperatures below 15000 K, and the values for mixing ratios 1%, 10%, 20% and 30% are almost the same.

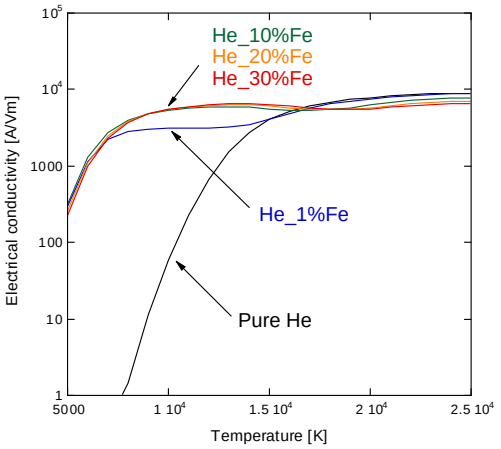

Fig. 2 Dependence of electrical conductivities of helium gas on temperature for each mixing ratio.

The other approximations, governing equations and boundary conditions are given in detail in our previous papers[4, 14]. The governing and auxiliary equations are solved iteratively by the SIMPLEC numerical procedure.

3. Calculation results

The present model is applied to the case of stationary helium TIG arc welding of stainless steel. Figure 3 shows the two-dimensional distribution of temperature and fluid flow velocity at a time 20 s after arc ignition, namely, when the weld pool has grown to a reasonable extent. Figure 4 shows the distributions of iron, chromium and manganese vapor in arc

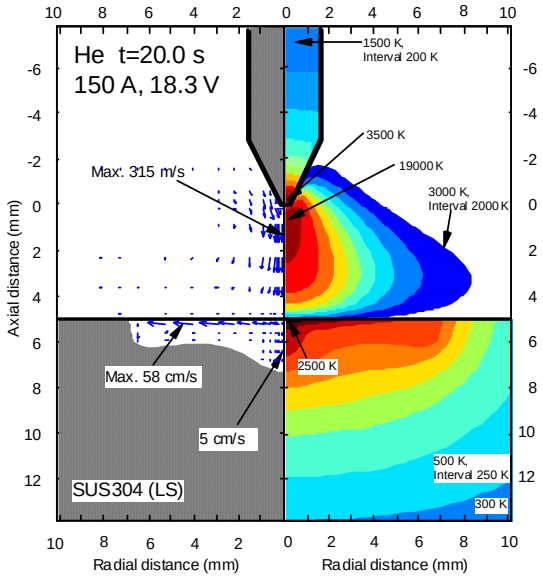

Fig. 3 Calculation result of helium GTA welding for a 150A at 20 seconds after arc ignition

plasma. The distributions of metal vapors depend on the diffusion term and the convection term, as described in Eq. (2). Due to the cathode jet, which leads to flow velocities of over 300 m/s in the welding arc, the convection term has a strong effect. Therefore, it is found that distribution of iron vapor expands in the radial direction and is concentrated around the weld pool surface.

Figure 4 shows the radial distribution of metal vapors around the anode surface. The concentrations of iron and chromium vapors are almost same and the maximum concentrations are about 4 mol%. The maximum concentration of manganese vapor is about 5 mol%. Due to the higher partial pressure of manganese vapor,

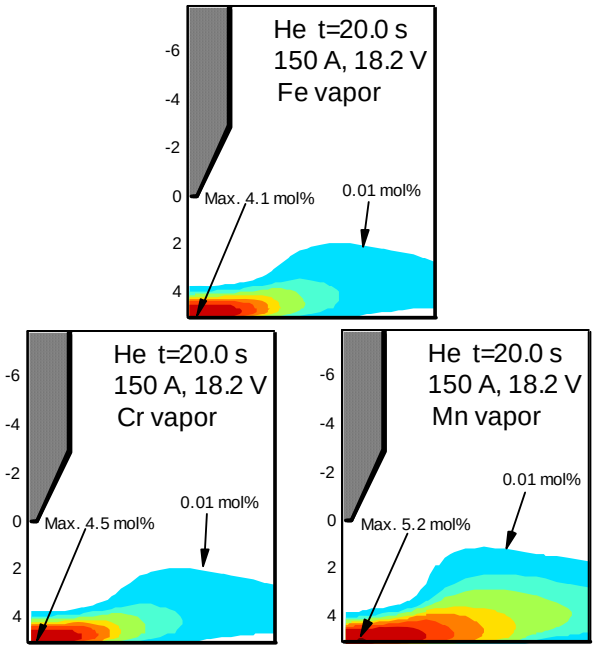

Fig. 4 Distribution of iron, chromium and manganese vapor in arc plasma

especially at low temperature, the concentration of manganese vapor is larger than those of iron and chromium vapors, despite the fact that the proportion of manganese in stainless steel is significantly smaller.

4. Conclusions

(1) A numerical model for stationary helium TIG arc welding taking into account the iron, chromium and manganese vapors produced from the weld pool surface have used to simulate the distribution of the metal vapors, plasma temperature, fluid flow velocity and the formation of the weld pool.

(2) Due to the cathode jet velocity of over 300 m/s in the welding arc, the convection term strongly affects the distributions of metal vapors. It was found that metal vapors expanded mainly in the radial direction and remained concentrated around the weld pool surface.

(3) The concentration of manganese vapor is larger than those of iron and chromium vapors, despite the fact that the proportion of manganese in stainless steel is significantly smaller.

Reference

1) M. Tanaka, T. Watanabe, T. Isa and H. Nishiwaki: New development of welding and thermal spraying, J. Plasma & Fusion Res., 82-8 (2006), 492-496 (in Japanese).
2) H.G. Fan and R. Kovacevic: The front line of modeling heat and mass transfer in arc welding processes, J. Japan Welding Soc., 76-2 (2007), 82-89.
3) H. Nishiyama, T. Sawada, H. Takana, M. Tanaka and M. Ushio: Computational simulation of arc melting process with complex interactions, ISIJ Int., 46-5 (2006), 705-711.
4) S. Tashiro, M. Tanaka, K. Nakata, T. Iwao, F. Koshiishi, K. Suzuki and K. Yamazaki: Plasma properties of helium gas tungsten arc with metal vapor, Sci. Technol. Weld. Join., 12-3 (2007), 202-207.
5) H.G. Fan and R. Kovacevic: A unified model of transport phenomena in gas metal arc welding including electrode, arc plasma and molten pool, J. Phys. D: Appl. Phys., 37 (2004), 2531-2544.
6) J. Menart and L. Lin: Numerical study of a free-burning argon arc with copper contamination from the anode, Plasma Chem. & Plasma Process., 19-2 (1999), 153-170.
7) K. Yamamoto, M. Tanaka, S. Tashiro, K. Nakata, K. Yamazaki, E. Yamamoto, K. Suzuki and A.B. Murphy: Metal vapour behaviour in thermal plasma of gas tungsten arcs during welding, Sci. Technol. Weld. Join., 13-6 (2008), 566-572.
8) H. Terasaki, M. Tanaka and M. Ushio: Effects of metal vapor on plasma state in helium gas tungsten arcs, Quarterly J. Japan Welding Soc., 20-2 (2002), 201-206.
9) M. Tanaka and J.J. Lowke: Predictions of weld pool profiles using plasma physics, J. Phys. D: Appl. Phys., 40 (2007), R1-R23.
10) C.R. Wilke: A viscosity equation for gas mixtures, J. Chem. Phys., 18-4 (1950), 517-519.
11) A.B. Murphy: A comparison of treatments of diffusion in thermal plasmas, J. Phys. D: Appl. Phys., 29 (1996), 1922-1932.
12) The Japan Institute of Metals: Edition No. 3 Data Book of Metals, MARUZEN CO., LTD, (1993) (in Japanese).
13) A.B. Murphy: Transport Coefficients of Air, Argon-Air, Nitrogen-Air, and Oxygen-Air Plasmas, Plasma Chemistry and Plasma Processing, 15-2 (1995), 279-307.
14) S. Tashiro, M. Tanaka, M. Nakatani, M. Furubayashi and Y. Yamazaki: Properties of Mass and Heat Transfer for Tube Cathode Arcs, Quarterly J. Japan Welding Soc., 25-1 (2007), 3-9 (in Japanese).